



Stimuli-Responsive Biomaterials

How to cite: Angew. Chem. Int. Ed. **2025**, e19925 doi.org/10.1002/anie.202519925

Boolean Logic-Based Controlled Release of Bioactive Proteins with Diversified Inputs

Murial L. Ross⁺, Ryan Gharios⁺, Shivani Kottantharayil⁺⁺, Annabella Li⁺⁺, and Cole A. DeForest*

Abstract: Stimuli-responsive biomaterials hold great promise in controlled therapeutic delivery, tissue engineering, and biosensing applications. Recently, molecular assembly via autonomous compilation has been employed to create topologically specified protein cargos that can be site-specifically tethered to and conditionally released from biomaterials following user-programmable Boolean logic. Prior implementation has been confined to simple fluorescent protein outputs and model protease inputs. In this manuscript, we extend the applicability of this framework by assembling all 7 unique logical operations emanating from a YES/OR/AND 3-input operator set to deliver bioactive proteins spanning diverse categories: growth factors (epidermal growth factor), model enzymes (β -lactamase, NanoLuciferase, and thioredoxin A), therapeutic nanobodies (anti-human epidermal growth factor receptor 2), de novo-engineered cytokines (Neoleukin), and fluorescent proteins (mGreenLantern). In so doing, we demonstrate programmable biomacromolecule release from material anchors in response to precise combinations of three orthogonal protease actuators while maintaining native bioactivity. Through inclusion of a photocleavable protein motif, we further establish that visible light can be employed as an additional input in specifying logic-based protein release. We anticipate these methods will powerfully expand opportunities for targeted therapeutic delivery and beyond.

Engineering control over protein presentation from biomaterials has advanced many applications such as controlled therapeutic release^[1-3] and organoid/tissue engineering.^[4,5] Toward this end, different groups have successfully deployed approaches co-opted from disparate disciplines (e.g., chemoenzymatic protein modification, nanotechnology, synthetic chemistry, others) and achieved remarkable synergies en route to engineering increasingly "smart" biomaterials and biohybrid constructs.^[6,7] However, while these endeavors have been promising, they routinely fall short of attaining a fully generalizable framework that allows for more sophisticated biocomputation. While the broader community has indeed found success in developing biomaterials with non-linear architectures that respond to multiple inputs such as protease, light, redox state, and small-molecule actuation, [8-11] these

examples often remain case-specific and tightly coupled to the designed application.

Towards imparting more modular Boolean biocomputability into materials, we recently demonstrated that molecular topology could be used to encode advanced environmental responsiveness. [12-14] In this manner, an executable YES gate is formed when a single stimuli-labile moiety links a biomolecular cargo and a stable material, an OR gate (denoted with logic symbol ∨) when two orthogonal scissile groups are connected in series, and an AND gate (denoted by logic symbol ∧) when two orthogonally cleavable linkers are included in parallel (Figure 1a–c). Hierarchical nesting of the YES, OR, and AND gates affords advanced logical circuits, whereby 7 functionally distinct response types can be generated for systems involving up to 3 inputs (Figure 1d).

[*] M. L. Ross⁺, S. Kottantharayil⁺⁺, C. A. DeForest Department of Bioengineering, University of Washington, Seattle, WA 98105, USA

E-mail: profcole@uw.edu

R. Gharios⁺, A. Li⁺⁺, C. A. DeForest

Department of Chemical Engineering, University of Washington, Seattle, WA 98105, USA

C. A. DeForest

Department of Chemistry, University of Washington, Seattle, WA 98105, USA

C. A. DeForest

Institute of Stem Cell & Regenerative Medicine, University of Washington, Seattle, WA 98109, USA

C. A. DeForest

Molecular Engineering & Sciences Institute, University of Washington, Seattle, WA 98105, USA

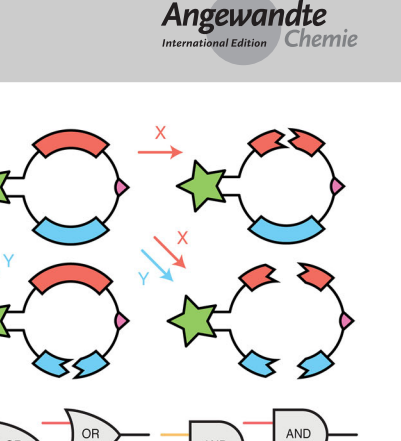
C. A. DeForest

Institute for Protein Design, University of Washington, Seattle, WA 98105, USA

- [++] Both authors contributed equally to this work.
- [⁺] Both are co-first authors.
- Additional supporting information can be found online in the Supporting Information section

a)

Communication



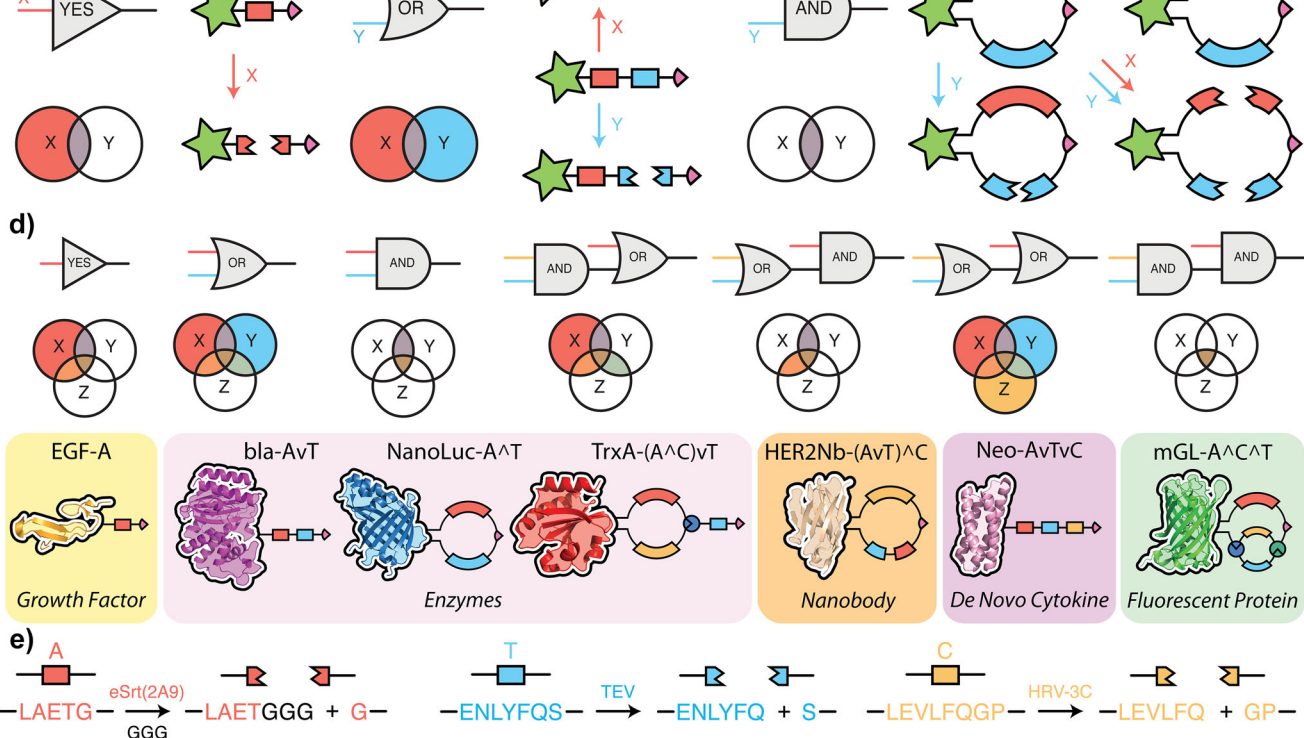


Figure 1. Autonomously compiled Boolean logic-responsive operators for delivery of diverse bioactive cargo. a) YES-gate, where a single input drives cleavage of a peptide backbone (colored rectangle) and protein (green star) release. The material-anchoring SpyTag is depicted as a pink wedge. b) OR-gate (logic symbol V), formed by two inputs in series. Only one input is needed to release cargo. c) AND-gate (\land logic symbol), where two inputs are in parallel and both must be present for release. d) All 7 possible nested logical operators with their associated cargo spanning diverse categories of proteins (i.e., growth factors, enzymes, nanobodies, de novo cytokines, fluorescent proteins). Each region of the Venn diagrams displayed represents a unique combination of protease inputs and indicates whether the tether is predicted to cleave (colored) or remain intact (white), e) Reactions depicting protease recognition of target sequence and subsequent cleavage: the recognition sequence LAET↓G (denoted as A) is recognized by eSrtA(2A9); ENLYFQ\S (denoted as T) by TEV; LEVLFQ\GP (denoted as C) by HRV-3C. (Adapted from Gharios et al., Nat. Chem. Bio., 2025.[15] Copyright 2025 Nature. Reproduced with permission).

Though engineered molecular topology has been exploited previously to gain Boolean control over small molecule, protein, and cell release from engineered biomaterials, [12-14] these prior approaches have almost exclusively relied on poorly scalable peptide chemistries protracted multi-step organic alongside syntheses. Sidestepping these limitations, we recently demonstrated that logically releasable protein cargos could be "autonomously compiled" in a single unsupervised synthetic step.[15] In this manner, topologically specified protein cargos are formed during recombinant expression via spontaneous intramolecular ligation, permitting direct and facile synthesis of functionally complex operators. Despite these advances, these initial studies were confined to model protease inputs and fluorescent protein cargos; questions concerning method generalizability, extension to therapeutically relevant proteins, and diversification of inputs remain.

b)

Toward answering these questions, we sought to extend our methods to 7 different bioactive protein cargos, each releasable via one of the 7 unique logical operations emanating from YES/OR/AND operators involving 3 orthogonal protease inputs. In this manner, we selected epi-

dermal growth factor (EGF) as a model growth factor, β-lactamase (bla), NanoLuciferase (NanoLuc)^[16] and thioredoxin A (TrxA) as model enzymes, an anti-human epidermal growth factor receptor 2 nanobody (HER2Nb) as a model therapeutic, [17] Neoleukin (Neo) as a de novo-designed cytokine and Interleukin-2 (IL-2) mimic, [18] and fluorescent protein mGreenLantern (mGL) (Figure 1d). For our choice of proteases, we employed the sortase transpeptidase eSrtA(2A9) variant that was evolved to recognize the distinct peptide substrate LAET \(G \) (referred to as A), [19] an evolved version of the potyviral tobacco etch virus (TEV) protease that acts upon ENLYFQ\S (referred to as T), [20,21] and the human rhinovirus-3C (HRV-3C) protease that recognizes LEVLFQ↓GP (referred to as C) (Figure 1e). [22] All three proteases recognize markedly distinct peptide sequences with minimal crosstalk.[15]

After identifying target bioactive proteins and input proteases, we designed the following expression plasmids for 7 distinct species, each containing a 6x-Histidine tag for nickel-nitrilotriacetic acid-assisted Immobilized Metal Affinity Chromatography (IMAC)-based purification and a SpyTag for covalent tethering to SpyCatcher-displaying materials^[23]:

15213773, 0, Downloaded from https://onlinelibrary.wiley.com/doi/10.1002/anie.202519925 by Cole DeForest - University Of Washington, Wiley Online Library on [10/11/2025]. See the Terms and Conditions (https://onlinelibrary.wiley.com/terms-and-conditions) on Wiley Online Library for rules of use; OA articles are governed by the applicable Creative Commons Licenses and Conditions on Wiley Online Library for rules of use; OA articles are governed by the applicable Creative Commons Licenses and Conditions on Wiley Online Library for rules of use; OA articles are governed by the applicable Creative Commons Licenses are governed by the applicable Creative Commons Library on [10/11/2025]. See the Terms and Conditions on Wiley Online Library wiley.

Communication

1) EGF-A: 2) bla-A∨T: 3) NanoLuc-A∧T, autonomously compiled through N-to-C cyclization using Split-intein circular ligation of proteins and peptides (SICLOPPS^[24,25]); 4) $TrxA-(A \land C) \lor T$, with tadpole-like topology formed via SnoopLigation of an N-terminal SnoopTag and an internal SnoopCatcher^[26]; 5) HER2Nb-(AVT)\(\triangle C\), cyclized via SICLOPPS^[24]; 6) Neo-A \vee T \vee C; and 7) mGL-A \wedge C \wedge T, engineered through tandem SnoopLigation and DogLigation reactions involving an N-terminal SnoopTag, a C-terminal DogTag, and the appropriate Catchers incorporated internally.[20] Routes of autonomous compilation and AlphaFold-based structural predictions for the final species are provided in the Supplementary Information. Plasmids were transformed into SHuffle T7 Competent Escherichia coli (E. Coli, New England Biolabs) and proteins expressed via standard protocols (See Supporting Information). Autonomously compiled protein species were purified by IMAC purification. To remove macrocylic byproducts, cyclic constructs were further purified by size exclusion chromatography (SEC). Final protein purity was assessed by sodium dodecyl sulfate-polyacrylamide gel electrophoresis (SDS-PAGE) and liquid chromatography mass spectrometry (LC-MS) (See Supporting Information). All species were obtained in high purity, with yields varying between 5 to 30 mg per L of expression.

With purified proteins in hand, we sought to assay the 7 constructs' logical response to each of the 8 possible input combinations of eSrtA(2A9), HRV-3C, and TEV (where inputs are respectively denoted as A, C, T) at non-kinetically limited endpoints (Figure 2a). Protease cleavage was visualized via SDS-PAGE, whereby variably intact species gave rise to alternative migration patterns. Gel densitometry was then performed to determine the percentage of cargo cleaved from the SpyTag in response to corresponding inputs (See Supporting Information). Owing to the presence of monocyclic impurities, gel densitometry-based analysis was not performed for mGL-A\C\T. For all other species, constructs cleaved following the pre-programmed logical operation regardless of cargo identity (Figure 2b–g).

Encouraged that logical cleavage proceeded as expected for all species, we next probed whether the intact or partially cleaved operators as well as fully released constructs maintained bioactivity. In this manner, EGF bioactivity was measured via a luminescent assay of a human embryonic kidney (HEK293T) reporter cell line that expresses firefly luciferase in response to the Serum Response Element (SRE), a genetic element that controls gene expression in the presence of growth factors (Figure 3a). bla function was quantified via enzymatic hydrolysis of nitrocefin, a chromogenic cephalosporin (Figure 3b). NanoLuc activity was determined via luminescence following furimazine addition (Figure 3c). TrxA bioactivity was determined through an insulin precipitation assay.[27] TrxA is an oxidoreductase that cleaves insulin disulfide bonds in the presence of dithiothreitol (DTT), resulting in solution turbidity (Figure 3d). HER2Nb activity was assessed through SK-BR-3 breast cancer cell growth suppression^[28-30] (Figure 3e). Neo bioactivity was determined via luminescence of an iLite IL-2 reporter cell line (Figure 3f). Finally, mGL's fluorescence

was taken as an indication of bioactivity (Figure 3g). Regardless of input combination, all species exhibited marked bioactivity compared with construct-free negative controls (Figure 3h-n); this indicates that cargo bioactivity is not impacted by the attached logical operator or fraction of remaining logical gate following differential proteolytic cleavage.

Heartened by the ability to control logical operations with complex cargos while maintaining bioactivity in solution, we turned our attention towards the functional release of species in a drug delivery-motivated material context. Here, we immobilized SpyCatcher-azide, whereby azido-phenylalanine is site-specifically incorporated near the protein's C-terminus via genetic code expansion, onto dibenzocyclooctyne (DBCO)-functionalized magnetic beads via strain-promoted azide-alkyne cycloaddition (SPAAC) (Figure 4a, see Supporting Information).[31] Following SpyLigation-mediated bead functionalization with each logically releasable cargo, responsiveness to all eight input combinations involving A, C, and T was evaluated. Protein release at non-kinetically limited endpoints was quantified using the aforementioned bioactivity assays on sample supernatant (Figure 4b). Excitingly, all samples behaved as expected, in that similar levels of bioactive protein were detected across all 7 species in their expected conditions following their preprogrammed logical responses (Figure 4c-i).

Having demonstrated the logic-based release of a variety of bioactive cargos using orthogonal proteases, we next sought to explore whether responsiveness to non-proteinaceous inputs could be encoded via autonomous molecular compilation. Inspired by previous work in our lab where we utilized a fully genetically encoded non-opsin optogenetic system to release proteins from stable gels^[32] and to degrade materials in response to light,[33] we identified the photocleavable green fluorescent protein PhoCl as a means to incorporate photoresponsiveness. Upon exposure to visible light (405 nm), PhoCl's chromophore undergoes a chemical rearrangement, irreversibly breaking its polypeptide backbone near its C-terminus (Figure 5a).[34,35] Here, we designed plasmids encoding an AND-gated mCherry construct, cyclized by SICLOPPS and containing a polyhistidine tag for IMAC purification and a SpyTag for material tethering, that was releasable upon exposure to both eSrtA(2A9) and light (See Supporting Information). Despite the comparatively complex structure, this species (denoted mCherry-PhoCl∧A) was obtained in high purity.

We first tested the logical operation of mCherry-PhoCl∧A by exposing the construct to all possible input combinations, then utilized SDS-PAGE and gel densitometry to determine logical operation (Figure 5b-c). We saw that up to 72% of the mCherry cargo was successfully released upon the addition of both inputs, with some off-target release upon the addition of input A, potentially due to premature cleavage of PhoCl from ambient light. In its linear form, the PhoCl variant used (PhoCl2c) has a reported dissociation efficiency of 92% [34]; we attributed the slightly reduced efficiency to cyclic strain on the C-terminal backbone. Excited that we achieved controlled release via two distinct input classes, we moved forward with mimicking drug delivery via solid support (Figure 5d).



15213773, 0, D

wnloaded from https://onlinelibrary.wiley.com/doi/10.1002/anie.202519925 by Cole DeForest - University Of Washington , Wiley Online Library on [10/11/2025]. See the Terms and Conditions (https://onlinelibrary.wiley.com/

conditions) on Wiley Online Library for rules of use; OA articles are governed by the applicable Creative Commons l

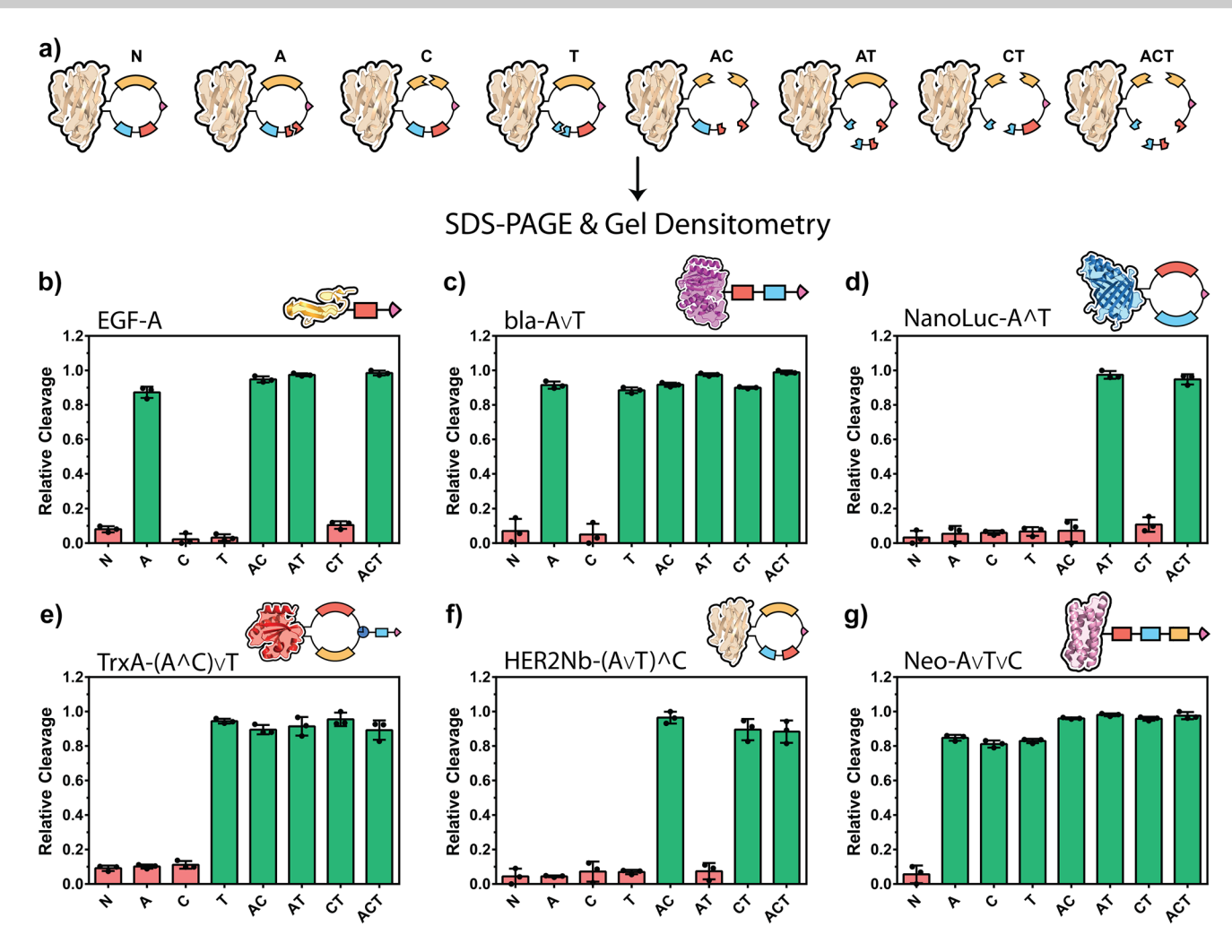


Figure 2. Validation of cargo release following Boolean logic. a) Logical operators are treated with all possible protease combinations wherein N indicates no treatment, A indicates eSrtA(2A9), C indicates HRV-3C, and T indicates TEV. Here, HER2Nb-(A \vee T) \wedge C demonstrates how logic gate conformation changes based on treatment. Protease-treated samples are analyzed via SDS-PAGE, whereby gel densitometry is performed to determine cleavage of cargo from the SpyTag. The response profiles of: b) EGF-A. Two-input c) bla-A \vee T and d) NanoLuc-A \wedge T. Three-input e) TrxA-(A \wedge C) \vee T, f) HER2Nb-(A \vee T) \wedge C, and g) Neo-A \vee T \vee C. The y-axis represents relative SpyTag cleavage from the cargo as measured through gel densitometry analysis; the x-axis indicates protease treatment conditions. Green bars indicate conditions expected to yield tether cleavage, whereas red bars indicate conditions not expected to yield cleavage. Error bars correspond to \pm 1 standard deviation about the mean with propagated uncertainties. See Supporting Information for gel images. All experiments were performed in triplicate (biological replicates, n=3).

Cargo was successfully delivered upon the addition of both inputs and with less than 30% off-target release. Although the delivery profiles had lower signal-to-noise ratios than previously demonstrated proteolytic cleavage, we successfully incorporated a new input that adds a new layer of input multiplexability. We anticipate that alternative inputs can be readily incorporated into these topologies, but the field is currently limited by available stimuli-responsive protein technologies that undergo full peptide backbone cleavage.

In conclusion, we demonstrated the extension of our autonomous molecular compilation-based approach to a broader palette of therapeutically relevant cargos (growth factors, enzymes, nanobodies, and de novo cytokines) while demonstrating that bioactivity is retained pre- and post-

release. Additionally, we diversified the array of potential inputs for logical response beyond simple proteases to newly include visible light. These systems allow us to multiplex distinct inputs onto bespoke frameworks that are fully genetically encoded and readily portable from lab-to-lab. Although this proof-of-concept study employs model proteases for cargo release, disease-relevant proteases (e.g., matrix metalloproteinases, cathepsins) could be easily substituted. We envision that these logical operators could be used to drive therapeutic release in a disease-directed manner or in combination with transdermal illumination. We anticipate this method will find widespread applicability in the development of next-generation biomaterials geared towards controlled release and regenerative medicine.

15213773, 0, Downloaded from https://onlinelibrary.wiley.com/doi/10.1002/anie.202519925 by Cole DeForest - University Of Washington , Wiley Online Library on [10/11/2025]. See the Terms and Conditions (https://onlinelibrary.wiley.com/doi/10.1002/anie.202519925 by Cole DeForest - University Of Washington , Wiley Online Library on [10/11/2025]. See the Terms and Conditions (https://onlinelibrary.wiley.com/doi/10.1002/anie.202519925 by Cole DeForest - University Of Washington , Wiley Online Library on [10/11/2025]. See the Terms and Conditions (https://onlinelibrary.wiley.com/doi/10.1002/anie.202519925 by Cole DeForest - University Of Washington , Wiley Online Library on [10/11/2025]. See the Terms and Conditions (https://onlinelibrary.wiley.com/doi/10.1002/anie.202519925 by Cole DeForest - University Of Washington , Wiley Online Library on [10/11/2025]. See the Terms and Conditions (https://onlinelibrary.wiley.com/doi/10.1002/anie.202519925 by Cole DeForest - University Of Washington , Wiley Online Library on [10/11/2025].

conditions) on Wiley Online Library for rules of use; OA articles are governed by the applicable Creative Commons License

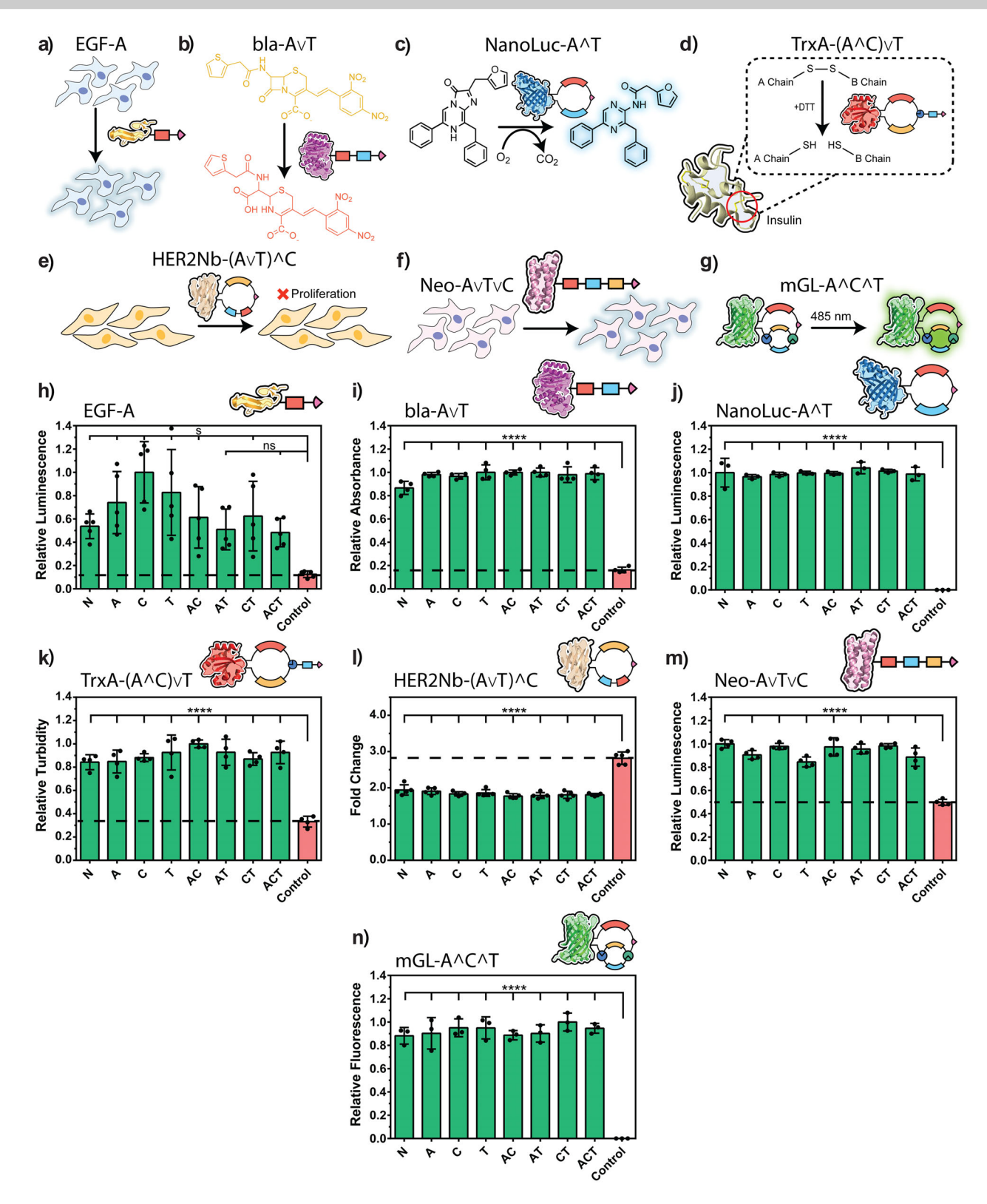


Figure 3. Bioactivity of cargo following in-solution treatment via protease actuators. Bioactivity was determined from the following assays: a) SRE HEK293T reporter line luminescence in response to EGF. b) Nitrocefin undergoes a color change when treated with bla. c) Furimazine luminescence when reacted with NanoLuc. d) TrxA cleaves the disulfide bonds in insulin, resulting in increased solution turbidity. e) HER2Nb suppresses SK-BR-3 cell proliferation. f) IL-2 reporter cell line luminescence in response to Neo. g) mGL fluorescence under 485 nm light. Bioactivity was observed for all conditions compared to negative controls: h) EGF (n = 5, N, AC, CT=*, A=***, T=****, C=*****). i) bla (n = 4). j) NanoLuc (n = 3). k) TrxA (n = 4). l) HER2Nb (n = 5). m) Neo (n = 4). n) mGL (n = 3). A indicates eSrtA(2A9), C indicates HRV-3C, and T indicates TEV. Error bars correspond to ± 1 standard deviation about the mean with propagated uncertainties. Number of technical replicates listed per construct. One-way ANOVA test with Tukey's Post-Hoc analysis comparing each condition to the control, α=0.05. *=p < 0.005, ***=p < 0.0005, ****=p < 0.0005, ****=p < 0.0005.

15213773, 0, Downloaded from https://onlinelibrary.wiley.com/doi/10.1002/anie.202519925 by Cole DeForest - University Of Washington , Wiley Online Library on [10/11/2025]. See the Terms and Conditions (https://onlinelibrary.wiley.com/doi/10.1002/anie.202519925 by Cole DeForest - University Of Washington , Wiley Online Library on [10/11/2025]. See the Terms and Conditions (https://onlinelibrary.wiley.com/doi/10.1002/anie.202519925 by Cole DeForest - University Of Washington , Wiley Online Library on [10/11/2025]. See the Terms and Conditions (https://onlinelibrary.wiley.com/doi/10.1002/anie.202519925 by Cole DeForest - University Of Washington , Wiley Online Library on [10/11/2025]. See the Terms and Conditions (https://onlinelibrary.wiley.com/doi/10.1002/anie.202519925 by Cole DeForest - University Of Washington , Wiley Online Library on [10/11/2025]. See the Terms and Conditions (https://onlinelibrary.wiley.com/doi/10.1002/anie.202519925 by Cole DeForest - University Of Washington , Wiley Online Library on [10/11/2025].

and-conditions) on Wiley Online Library for rules of use; OA articles are governed by the applicable Creative Commons License

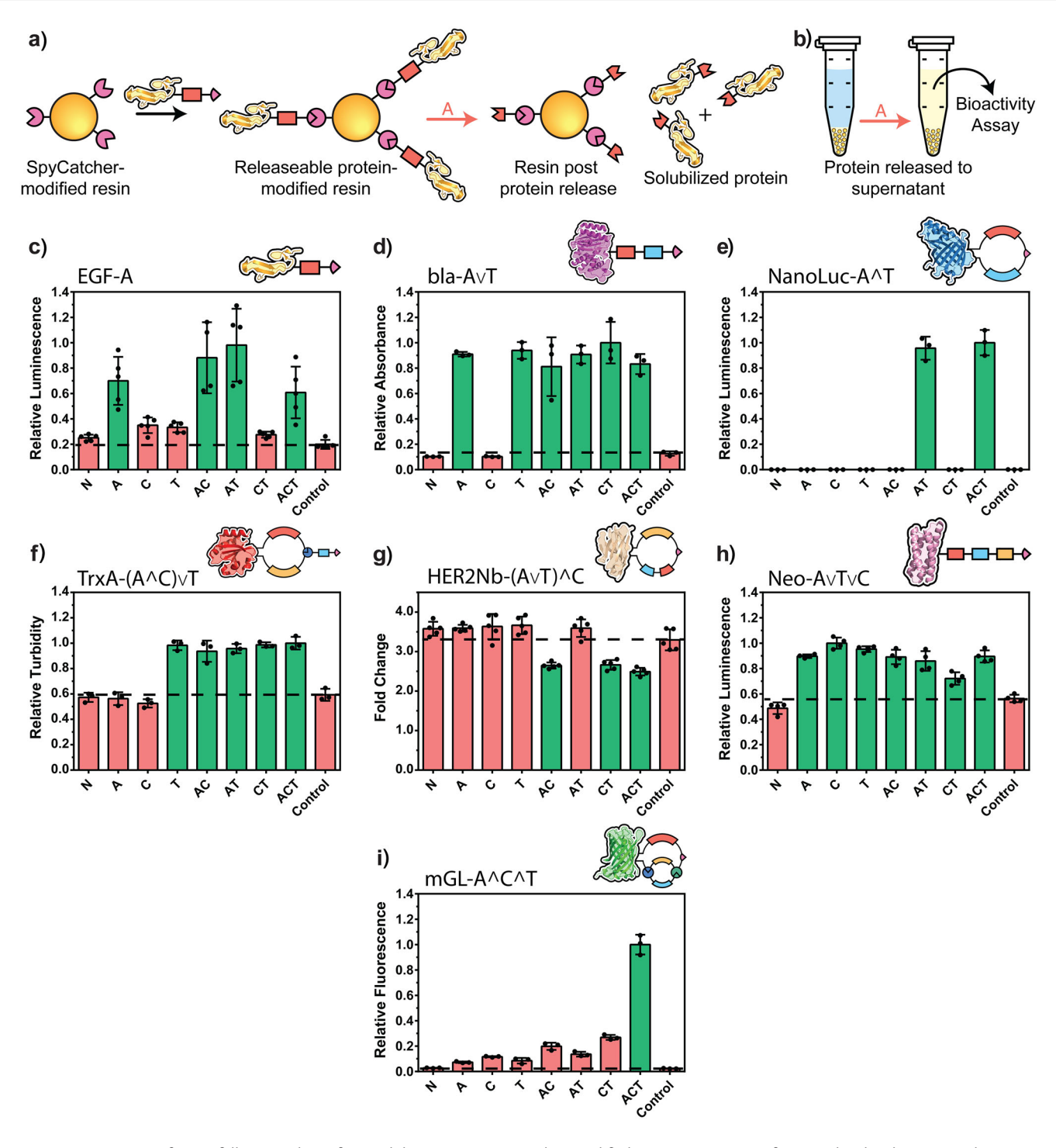


Figure 4. Bioactivity of cargo following release from solid support. a) SpyCatcher-modified magnetic resin was functionalized with SpyTagged protein, shown here as EGF-A. Resin was treated with all possible protease combinations, with cargo releasing according to the attached logical operator. b) Released protein was sampled from the supernatant for bioactivity assays. Bioactivity was observed for conditions expected to yield release, otherwise unreleased species exhibited similar responses to the negative control: c) Luminescence from EGF-treated SRE HEK293T reporter line (n = 5). d) Absorbance of nitrocefin when treated with bla (n = 3). e) NanoLuc luminescence (n = 3). f) Turbidity of insulin solution from TrxA, indicating disulfide bond cleavage (n = 3). g) Fold change in SK-BR-3 cell proliferation. Growth suppression was observed when treated with HER2Nb (n = 5). h) Luminescence of IL-2 reporter cell line in response to Neo (n = 4). i) Fluorescence of mGL (n = 3). A indicates eSrtA(2A9), C indicates HRV-3C, and T indicates TEV. Green bars indicate conditions expected to yield release, whereas red bars indicate conditions not expected to yield release. Error bars correspond to ± 1 standard deviation about the mean with propagated uncertainties. Number of technical replicates listed per construct.

15213773, 0, D

wnloaded from https://onlinelibrary.wiley.com/doi/10.1002/anie.202519925 by Cole DeForest - University Of Washington , Wiley Online Library on [10/11/2025]. See the Terms

and Conditions (https

conditions) on Wiley Online Library for rules of use; OA articles are governed by the applicable Creative Commons

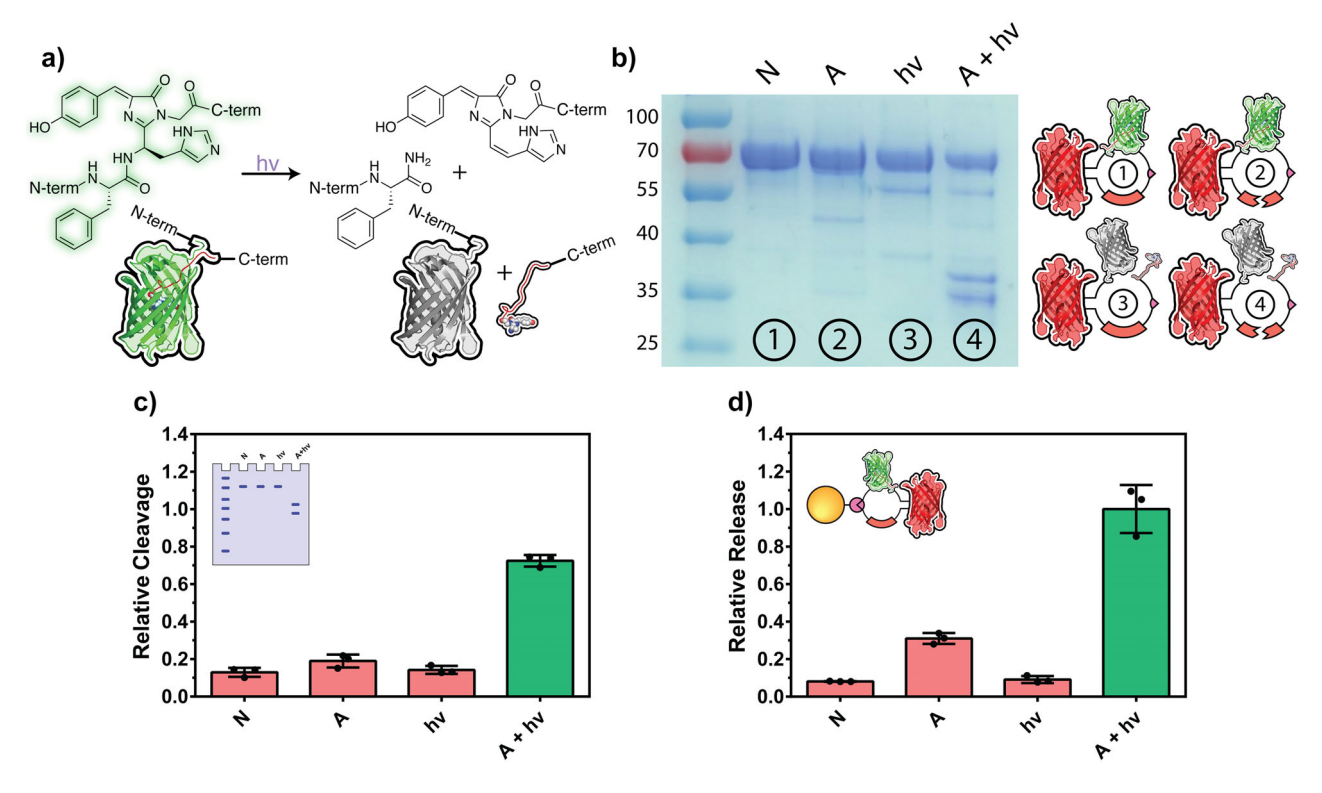


Figure 5. Controlled release of protein cargo via photoscission and proteolytic cleavage. a) Under 405 nm light, the PhoCl chromophore rearranges, resulting in the breakage of the peptide backbone. b) mCherry-PhoCl \land A was treated with all possible conditions and visualized by SDS-PAGE (lanes left to right: N, A, hv, A + hv). Protein stickers correspond to predicted cleavage and release of cargo. Release of mCherry-PhoCl \land A was analyzed via c) gel densitometry (biological replicates, n=3), and d) release from functionalized magentic beads (technical replicates, n=3). Green bars indicate conditions expected to yield release, whereas red bars indicate conditions not expected to yield release. A indicates eSrtA(2A9), hv indicates treatment with 405 nm light. Error bars correspond to ± 1 standard deviation about the mean with propagated uncertainties.

Acknowledgements

The authors thank R. Francis and A. Garcia for collaborating on designing and validating the SpyCatcher-azide, J. Davis for gifting HEK293T cells (previously obtained from ATCC, CRL-3216), A. O'Brian for her guidance on protein visualization, and J. Hoye for support on stable cell line generation. Part of this work was conducted with instrumentation provided by the Joint Center for Deployment and Research in Earth Abundant Materials (JCDREAM). Additionally, the authors gratefully acknowledge Dale Whittington for training and maintenance of the UW Mass Spectrometry Center. This work was supported by a grant (DMR 1807398, C.A.D.) from the National Science Foundation and a Maximizing Investigators' Research Award (R35GM138036, C.A.D.) from the National Institutes of Health. Student support was further provided through the National Science Foundation (DGE-2140004, M.L.R.), Goldwater Scholarships (A.L., S.P.K.), and a University of Washington Mary Gates Endowment for Students (S.P.K.).

Conflict of Interests

C.A.D., R.G., and M.L.R. have filed a patent application (PCT/US2025/031504) related to the work described in this article. The other authors declare no conflict of interest.

Data Availability Statement

The data that support the findings of this study are available in the Supporting Information of this article.

Keywords: Bioactive therapeutics • Boolean logic • Drug delivery • Protein engineering • Stimuli-responsive

- O. S. Fenton, K. N. Olafson, P. S. Pillai, M. J. Mitchell, R. Langer, Adv. Mater. 2018, 30, 1705328. https://doi.org/10.1002/adma.201705328.
- [2] J. Li, D. J. Mooney, Nat. Rev. Mater. 2016, 1. https://doi.org/10. 1038/natreymats.2016.71.
- [3] J. Gao, J. M. Karp, R. Langer, N. Joshi, *Chem. Mater.* 2023, 35, 359–363, https://doi.org/10.1021/acs.chemmater.2c03003.
- [4] C. A. DeForest, K. S. Anseth, Annu. Rev. Chem. Biomol. Eng. 2012, 3, 421–444, https://doi.org/10.1146/annurev-chembioeng-062011-080945.
- [5] M. Hofer, M. P. Lutolf, Nat. Rev. Mater. 2021, 6, 402–420, https://doi.org/10.1038/s41578-021-00279-y.
- [6] A. R. Narkar, Z. Tong, P. Soman, J. H. Henderson, *Biomaterials* 2022, 283, 121450. https://doi.org/10.1016/j.biomaterials.2022. 121450.
- [7] R. Gharios, R. M. Francis, C. A. DeForest, *Matter* 2023, 6, 4195–4244, https://doi.org/10.1016/j.matt.2023.10.012.
- [8] E. R. Ruskowitz, C. A. DeForest, Nat. Rev. Mater. 2018, 3, 1–17, https://doi.org/10.1038/natrevmats.2017.87.



1521 3773, 0, Downloaded from https://onlinelibrary.wiley.com/doi/10.1002/anie.202519925 by Cole DeForest - University Of Washington , Wiley Online Library on [10/11/2025]. See the Terms and Conditions (https://onlinelibrary.wiley.com/doi/10.1002/anie.202519925 by Cole DeForest - University Of Washington , Wiley Online Library on [10/11/2025]. See the Terms and Conditions (https://onlinelibrary.wiley.com/doi/10.1002/anie.202519925 by Cole DeForest - University Of Washington , Wiley Online Library on [10/11/2025]. See the Terms and Conditions (https://onlinelibrary.wiley.com/doi/10.1002/anie.202519925 by Cole DeForest - University Of Washington , Wiley Online Library on [10/11/2025]. See the Terms and Conditions (https://onlinelibrary.wiley.com/doi/10.1002/anie.202519925 by Cole DeForest - University Of Washington , Wiley Online Library on [10/11/2025].

and-conditions) on Wiley Online Library for rules of use; OA articles are governed by the applicable Creative Commons

- [9] A. Gelmi, C. E. Schutt, Adv. Healthcare Mater. 2021, 10, 2001125. https://doi.org/10.1002/adhm.202001125.
- [10] Z. Fu, L. Ouyang, R. Xu, Y. Yang, W. Sun, *Mater. Today* 2022, 52, 112–132, https://doi.org/10.1016/j.mattod.2022.01.001.
- [11] V. Stein, M. Nabi, K. Alexandrov, ACS Synth. Biol. 2017, 6, 1337–1342, https://doi.org/10.1021/acssynbio.6b00370.
- [12] P. M. Gawade, J. A. Shadish, B. A. Badeau, C. A. DeForest, Adv. Mater. 2019, 31, 1902462. https://doi.org/10.1002/adma. 201902462.
- [13] E. R. Ruskowitz, M. P. Comerford, B. A. Badeau, C. A. DeForest, *Biomater. Sci.* 2019, 7, 542–546, https://doi.org/10. 1039/C8BM01304G.
- [14] B. A. Badeau, M. P. Comerford, C. K. Arakawa, J. A. Shadish, C. A. DeForest, *Nat. Chem.* 2018, 10, 251–258, https://doi.org/10. 1038/nchem.2917.
- [15] R. Gharios, M. L. Ross, A. Li, S. P. Kottantharayil, J. Hoye, C. A. DeForest, *Nat. Chem. Biol.* 2025, https://doi.org/10.1038/s41589-025-02037-5.
- [16] M. P. Hall, J. Unch, B. F. Binkowski, M. P. Valley, B. L. Butler, M. G. Wood, P. Otto, K. Zimmerman, G. Vidugiris, T. Machleidt, M. B. Robers, H. A. Benink, C. T. Eggers, M. R. Slater, P. L. Meisenheimer, D. H. Klaubert, F. Fan, L. P. Encell, K. V. Wood, ACS Chem. Biol. 2012, 7, 1848–1857, https://doi.org/10.1021/cb3002478.
- [17] I. Vaneycken, N. Devoogdt, N. Van Gassen, C. Vincke, C. Xavier, U. Wernery, S. Muyldermans, T. Lahoutte, V. Caveliers, FASEB J. 2011, 25, 2433–2446, https://doi.org/10.1096/fj.10-180331
- [18] D.-A. Silva, S. Yu, U. Y. Ulge, J. B. Spangler, K. M. Jude, C. Labão-Almeida, L. R. Ali, A. Quijano-Rubio, M. Ruterbusch, I. Leung, T. Biary, S. J. Crowley, E. Marcos, C. D. Walkey, B. D. Weitzner, F. Pardo-Avila, J. Castellanos, L. Carter, L. Stewart, S. R. Riddell, M. Pepper, G. J. L. Bernardes, M. Dougan, K. C. Garcia, D. Baker, *Nature* 2019, 565, 186–191, https://doi.org/10.1038/s41586-018-0830-7.
- [19] B. M. Dorr, H. O. Ham, C. An, E. L. Chaikof, D. R. Liu, *Proc. Natl. Acad. Sci* 2014, 111, 13343–13348, https://doi.org/10.1073/pnas.1411179111.
- [20] A. H. Keeble, V. K. Yadav, M. P. Ferla, C. C. Bauer, E. Chuntharpursat-Bon, J. Huang, R. S. Bon, M. Howarth, *Cell Chem. Biol.* 2022, 29, 339–350.e10, https://doi.org/10.1016/j.chembiol.2021.07.005.
- [21] L. D. Cabrita, D. Gilis, A. L. Robertson, Y. Dehouck, M. Rooman, S. P. Bottomley, *Protein Sci.* 2007, 16, 2360–2367, https://doi.org/10.1110/ps.072822507.

- [22] E. H. Abdelkader, G. Otting, J. Biotechnol. 2021, 325, 145–151, https://doi.org/10.1016/j.jbiotec.2020.11.005.
- [23] B. Zakeri, J. O. Fierer, E. Celik, E. C. Chittock, U. Schwarz-Linek, V. T. Moy, M. Howarth, *Proc. Natl. Acad. Sci* 2012, 109, E690–E697, https://doi.org/10.1073/pnas.1115485109.
- [24] A. Tavassoli, S. J. Benkovic, Nat. Protoc. 2007, 2, 1126–1133, https://doi.org/10.1038/nprot.2007.152.
- [25] A. J. Stevens, Z. Z. Brown, N. H. Shah, G. Sekar, D. Cowburn, T. W. Muir, J. Am. Chem. Soc. 2016, 138, 2162–2165, https://doi. org/10.1021/jacs.5b13528.
- [26] G. Veggiani, T. Nakamura, M. D. Brenner, R. V. Gayet, J. Yan, C. V. Robinson, M. Howarth, *Proc. Natl. Acad. Sci. USA* 2016, 113, 1202–1207, https://doi.org/10.1073/pnas.1519214113.
- [27] A. Holmgren, J. Biol. Chem. 1979, 254, 9627–9632, https://doi. org/10.1016/S0021-9258(19)83562-7.
- [28] X. Liu, L. Luan, X. Liu, D. Jiang, J. Deng, J. Xu, Y. Yuan, J. Xing, B. Chen, D. Xing, H. Huang, Front. Immunol. 2023, 14, 1292839. https://doi.org/10.3389/fimmu.2023.1292839.
- [29] M. Pruszynski, M. D'Huyvetter, F. Bruchertseifer, A. Morgenstern, T. Lahoutte, Mol. Pharmaceutics 2018, 15, 1457–1466, https://doi.org/10.1021/acs.molpharmaceut.7b00985.
- [30] S. Burgstaller, T. R. Wagner, H. Bischof, S. Bueckle, A. Padamsey, D. Frecot, P. D. Kaiser, D. Skrabak, R. Malli, R. Lukowski, U. Rothbauer, iScience 2022, 25, 104907. https://doi.org/10.1016/j.isci.2022.104907.
- [31] N. J. Agard, J. A. Prescher, C. R. Bertozzi, J. Am. Chem. Soc. 2004, 126, 15046–15047, https://doi.org/10.1021/ja044996f.
- [32] J. A. Shadish, A. C. Strange, C. A. DeForest, J. Am. Chem. Soc. 2019, 141, 15619–15625, https://doi.org/10.1021/jacs.9b07239.
- [33] N. E. Gregorio, F. Zhang, Y. Suita, L. S. Ang, O. Prado, A. Fasuyi, J. M. Olson, K. R. Stevens, C. A. DeForest, *Sci. Adv.* 2025, 11, eadx3472. https://doi.org/10.1126/sciadv.adx3472.
- [34] X. Lu, Y. Wen, S. Zhang, W. Zhang, Y. Chen, Y. Shen, M. J. Lemieux, R. E. Campbell, *Chem. Sci.* **2021**, *12*, 9658–9672, https://doi.org/10.1039/D1SC01059J.
- [35] W. Zhang, A. W. Lohman, Y. Zhuravlova, X. Lu, M. D. Wiens, H. Hoi, S. Yaganoglu, M. A. Mohr, E. N. Kitova, J. S. Klassen, P. Pantazis, R. J. Thompson, R. E. Campbell, *Nat. Methods* 2017, 14, 391–394, https://doi.org/10.1038/nmeth.4222.

Manuscript received: September 10, 2025 Revised manuscript received: October 21, 2025 Manuscript accepted: October 23, 2025

Version of record online: ■■, ■